Supplemental Information

Supplemental Figures and Legends

Tasca et al. Fig. S1

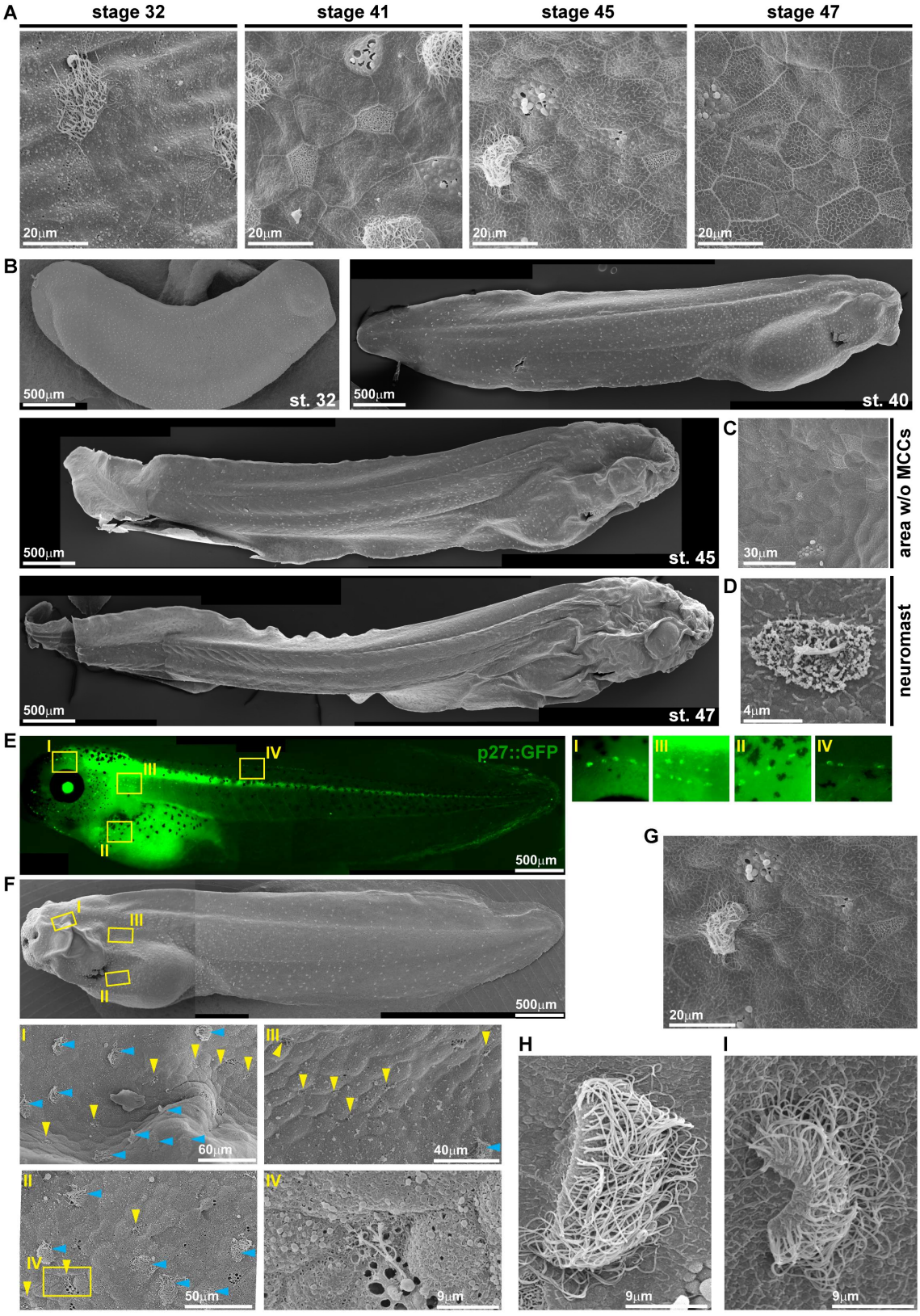

Supplemental Figure S1. (Related to Figure 1)

(A-D) Original micrographs used for characterization of epidermal MCC loss during *Xenopus* development in Fig. 1. Non pseudo-colored scanning electron micrographs from developmental stages 32 through 47. Cf. Fig. 1. **(A)** Analysis of the changing composition of mucociliary cell types in the epidermis shows progressive loss of MCCs, while ionocytes (ISCs), small secretory cells (SSCs) and mucus-secreting Goblet cells remain present. **(B)** Analysis of MCC-loss patterns on whole tadpoles. Images were reconstructed from multiple individual micrographs. **(C)** Magnification of skin area devoid of MCCs at stage (st.) 45 reveals presence of lateral line neuromast. **(D)** Magnified image of a neuromast. **(E-I)** Local loss of MCCs coincides with the emergence of the lateral line. **(E,F)** Correlative light and electron microscopy (CLEM) analysis of p27 promotor-driven GFP (p27::GFP) transgenic tadpole identifies GFP expression in *Xenopus* neuromasts of the lateral line system. Images were reconstructed from multiple individual micrographs. N = 1 embryo. **(E)** Fluorescent light microscopy image depicts GFP expression. Yellow boxes indicate location of magnified images. **(F)** Scanning electron micrographs of the same tadpole depicted in E confirm presence of neuromasts (yellow arrowheads) in locations of GFP expression. Yellow boxes indicate location of magnified images. Blue arrowheads indicate MCCs. **(G-I)** Scanning electron micrographs of areas with reduced ciliation **(G)** reveal MCCs with normal **(H)** and abnormal **(I)** morphology, indicating shedding of MCCs from the epithelium. (H) N = 4 MCCs. (I) N = 7 MCCs. Images in B,E,F were reconstructed from multiple individual micrographs.

Tasca et al. Fig. S2

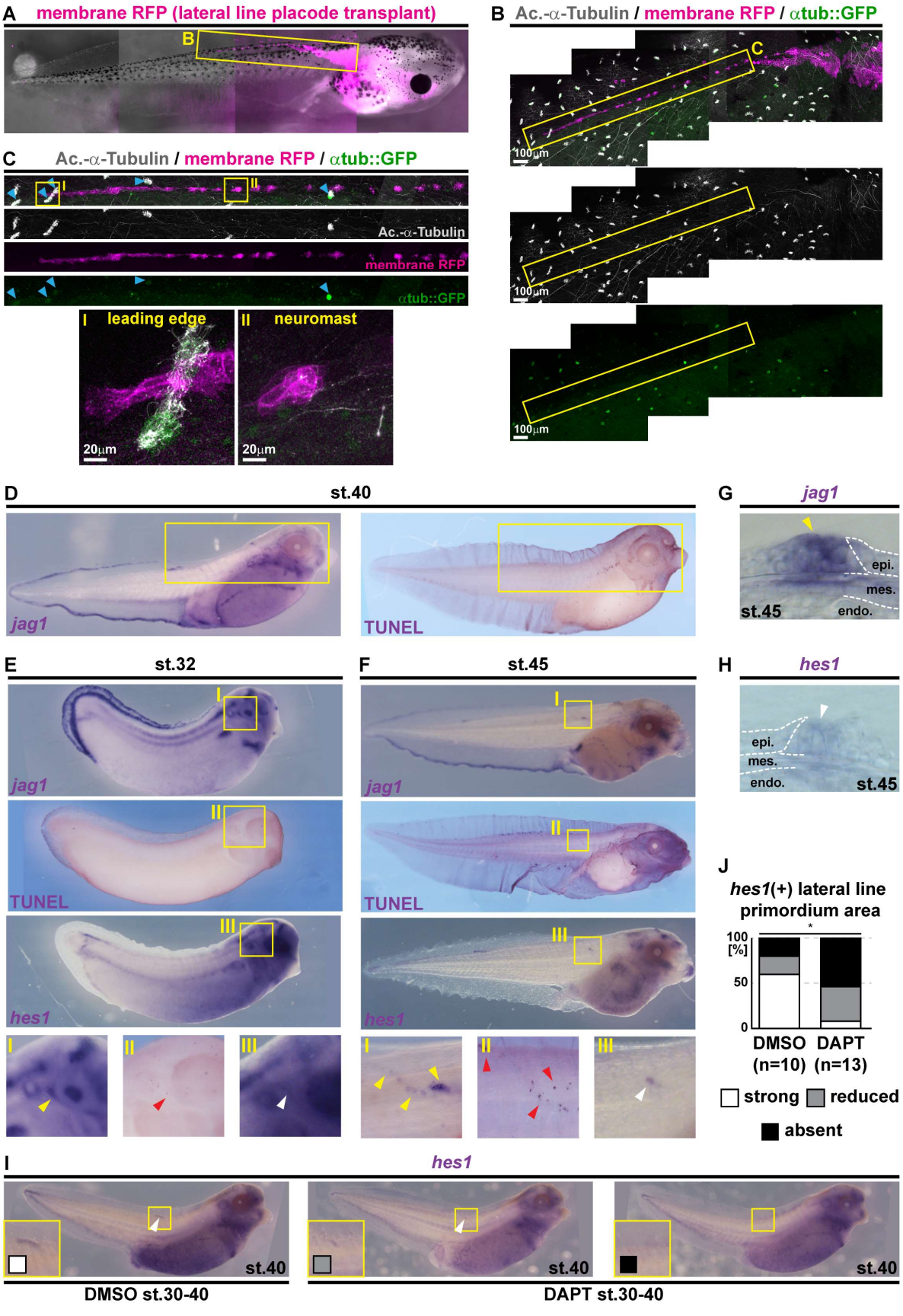

Supplemental Figure S2. (Related to Figure 1 and 2)

Local loss of MCCs correlates with neuromast emergence, Notch signaling and induction of apoptosis. **(A-C)** Micrographs of transplanted lateral line primordium and neuromasts (marked by membrane-RFP) reveal loss of MCCs (marked by α-tubulin promotor-driven GFP [αtub::GFP, green] and Acetylated-α-Tubulin [Ac.-α-Tubulin, grey] antibody staining) in areas where neuromasts have emerged. Images were reconstructed from multiple individual micrographs. **(A)** Fluorescent light microscopy image depicts whole tadpole at stage 45 which received a membrane RFP-labeled transplant of a lateral line primordium at st. 18. Yellow box indicates location used for confocal micrograph in B. N = 2. **(B-C)** Confocal micrograph of area depicted in A. Yellow boxes in B indicate the image area depicted in C. **(C)** Loss of MCCs in areas where neuromasts have emerged, but presence of MCCs above the lateral line primordium leading edge. Blue arrowheads indicate GFP(+) MCCs. **(D-J)** *In situ* hybridization and TUNEL staining shows Notch ligand expression (*jagged1*; *jag1*) and signaling (*hes1*) activity in the lateral line and apoptotic cells (TUNEL) along the lateral line migration path. **(D)** *jag1* and TUNEL staining (purple) in stage 40 tadpoles. Yellow boxes indicate location of magnified images in Fig. 2 B,C. *jag1* N = 3 embryos; TUNEL N = 13 embryos (same as in Figure 2B and C). **(E)** *jag1*, *hes1* and TUNEL staining (purple) in stage 32 tailbud embryos at the onset of lateral line placode migration. Yellow boxes indicate location of magnified images. *jag1* N = 5; TUNEL N = 6; *hes1* N = 7 embryos (same as in Supplemental Figure S4B and E). **(F)** *jag1*, *hes1* and TUNEL staining (purple) in stage 45 tadpoles. Yellow boxes indicate location of magnified images. *jag1* N = 3; TUNEL N = 7; *hes1* N = 8 embryos (same as in Supplemental Figure S4B and E). **(G-H)** Sections of neuromasts after *in situ* hybridization staining for *jag1* **(G)** and *hes1* **(H)** at stage 45. (G) N = 2 embryos. (H) N = 2 embryos. **(I-J)** *In situ* hybridization **(I)** and quantification **(J)** shows *hes1* (purple) expression after control treatment (DMSO) and after treatment with the Notch signaling inhibitor DAPT, demonstrating active Notch signaling close to the leading edge of the lateral line migration area at stage 40. Yellow boxes indicate location of magnified images. χ^2 test, * $P < 0.05$.

Tasca et al. Fig. S3

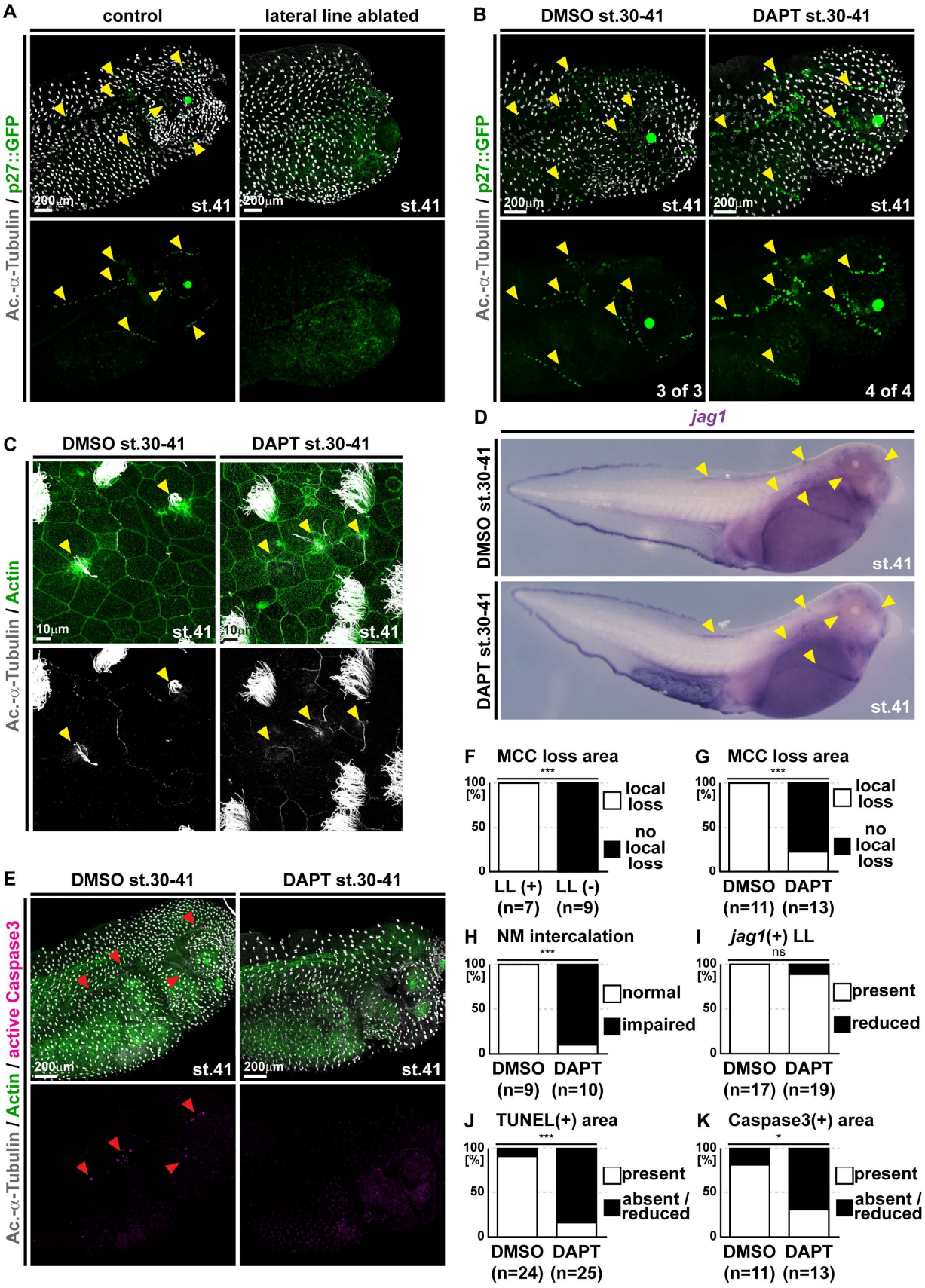

Supplemental Figure S3. (Related to Figure 2)

Notch signaling inhibition prevents MCC apoptosis, epidermal neuromast intercalation, but not lateral line migration and *jag1* expression. **(A-C,E)** Confocal micrographs, **(D)** in situ hybridization staining, and **(F-K)** quantification of results. **(A)** Ablation of the lateral line primordium at stage 28-30 prevents local loss of MCCs (Ac.-α-Tubulin, grey) and neuromast deposition (yellow arrowheads) in p27 promotor-driven GFP (p27::GFP; green) transgenic tadpoles at stage 41. **(B,C)** Notch signaling inhibition by DAPT application does not prevent lateral line migration and neuromast deposition (yellow arrowheads) **(B)**, but prevents lateral line induced MCC loss and neuromast (yellow arrowheads) intercalation **(C)**. F-actin (Actin, green) was used as counterstain in confocal images. Please note impaired neuromast spacing in DAPT treated tadpoles. **(D)** *In situ* hybridization shows unaffected *jag1* (purple) expression in the lateral line primordium and in neuromasts in control (DMSO) and DAPT treated tadpoles at stage 41. Yellow arrowheads indicate the lateral line migratory paths. **(E)** Active (cleaved) Caspase 3 positive cells (magenta; red arrowheads) are present along the lateral line migration paths in control (DMSO) treated embryos, but strongly reduced after DAPT treatment at stage 41. MCCs (Ac.-α-Tubulin, grey), F-actin (green). Pictures in A,B and E were reconstructed from multiple images. **(F)** Quantification of local MCC loss in controls (LL+) and lateral line ablated (LL-) embryos. χ^2 test, *** $P < 0.001$. **(G)** Quantification of local MCC loss in control (DMSO) and DAPT treated tadpoles. χ^2 test, *** $P < 0.001$. **(H)** Quantification of neuromast intercalation in control (DMSO) and DAPT treated tadpoles. χ^2 test, *** $P < 0.001$. **(I)** Quantification of *jag1* expression in control (DMSO) and DAPT treated tadpoles. χ^2 test, $P > 0.05$ = not significant. **(H)** Quantification of lateral line induced apoptosis (TUNEL staining, purple) in control (DMSO) and DAPT treated tadpoles. χ^2 test, *** $P < 0.001$. **(K)** Quantification of active Caspase 3 stained areas in control (DMSO) and DAPT treated tadpoles. χ^2 test, * $P < 0.05$.

Tasca et al. Fig. S4

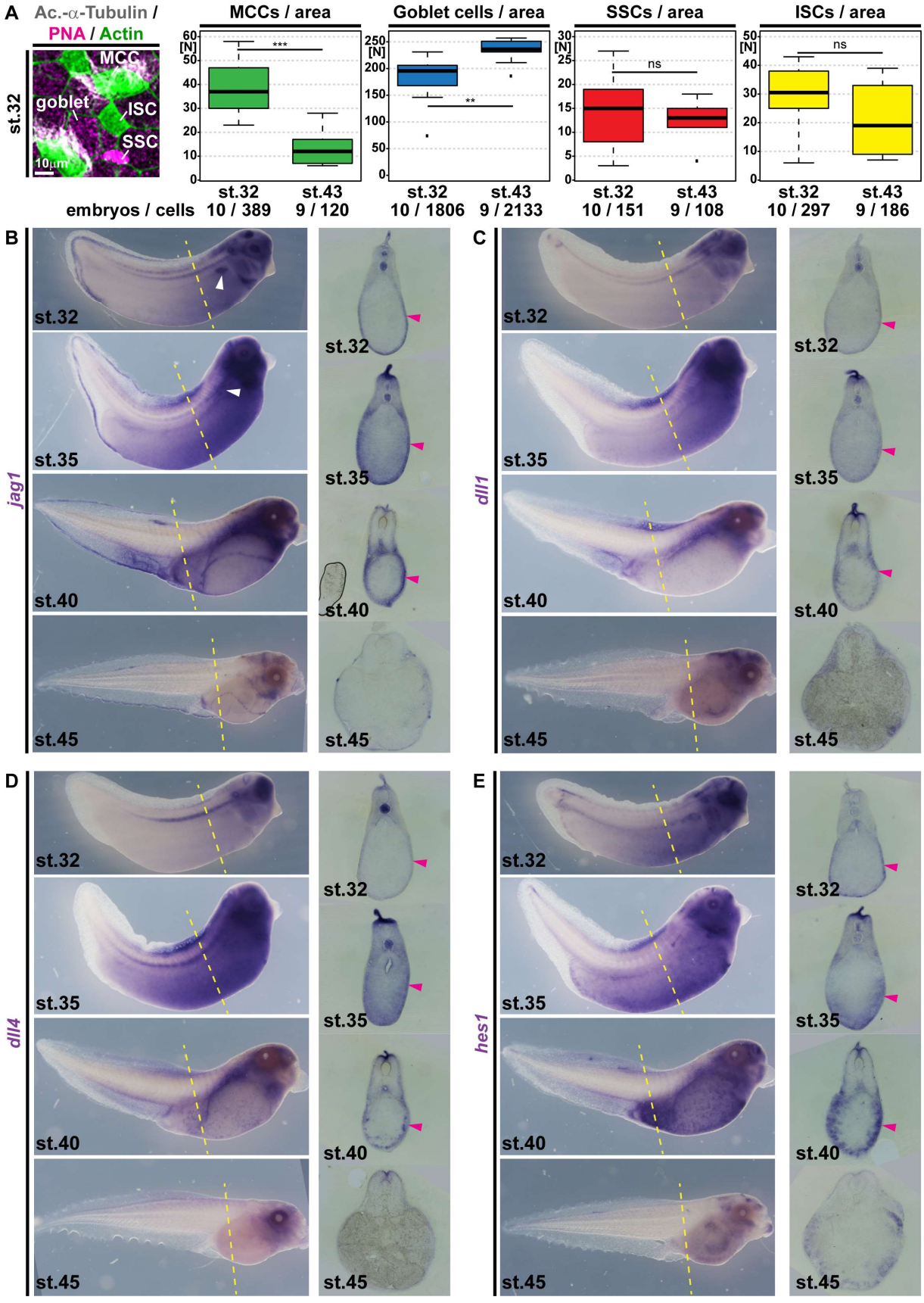

Supplemental Figure S4. (Related to Figure 3)

(A) Identification and quantification of epidermal cell types using confocal micrographs at stages 32 and 43. Cilia (Ac.-α-Tubulin, grey), mucus (PNA, magenta), F-actin (Actin, green). Quantification reveals significantly reduced numbers of MCCs and significantly increased numbers of Goblet cells at st. 43, but no significant change in SSC and ISC numbers. Mann Whitney test, ns $P > 0.05$ = not significant (ns), ** $P < 0.01$, *** $P < 0.001$.

(B-E) Expression analysis of Notch ligands *jag1*, *dll1* and *dll4*, and the Notch target *hes1*. Whole mount *in situ* hybridization was conducted on specimens from the same batches for all four genes in stages 32 to 45. Histological sections reveal distribution of signals among various tissues. Planes of sections in B-E are indicated by yellow dashed lines. **(B-D)** The expression of the Notch ligands *jag1*, *dll1* and *dll4* in mesodermal tissues underlying the epidermis (magenta arrowheads) increases between st. 32 and st. 35, is maintained at high levels at st. 40, and decreases by st. 45, i.e. after trans-differentiation of MCCs is largely completed. (B) st. 32 N = 5; st. 35 N = 3; st. 40 N = 3; st 45 N = 3 embryos. (C) st. 32 N = 9; st. 35 N = 3; st. 40 N = 4; st 45 N = 6 embryos. (D) st. 32 N = 5; st. 35 N = 3; st. 40 N = 4; st 45 N = 3 embryos. **(E)** The expression of the Notch target *hes1* in mesodermal tissues as well as in the epidermis (magenta arrowheads) increases between st. 32 and st. 35, is maintained at high levels at st. 40, and decreases by st. 45. st. 32 N = 7; st. 35 N = 4; st. 40 N = 8; st 45 N = 8 embryos. Please also note strong expression of *jag1* **(B)** in the developing pronephros (white arrowheads).

Tasca et al. Fig. S5

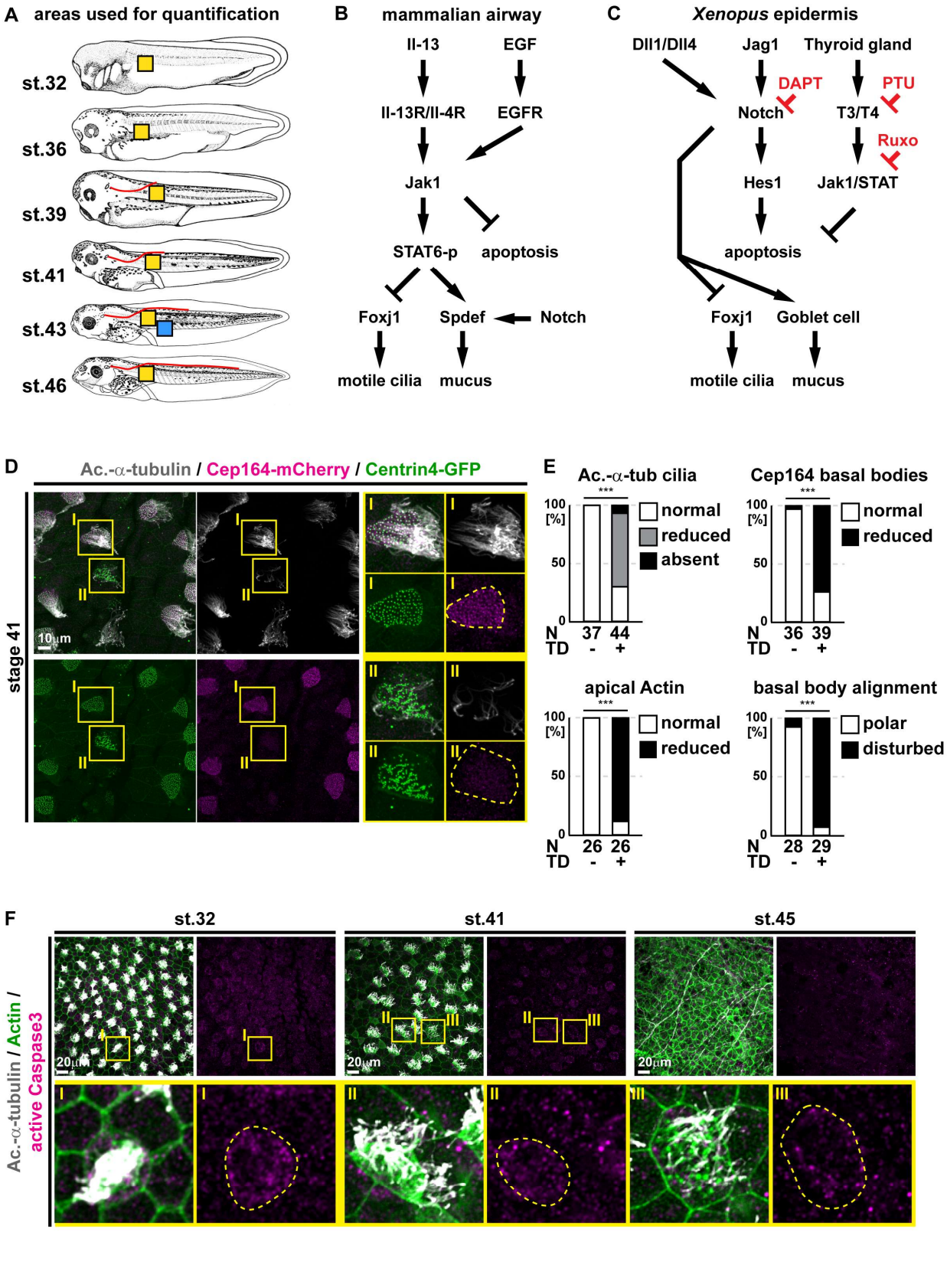

Supplemental Figure S5. (Related to Figure 3 and 5)

Global loss of MCCs through trans-differentiation into Goblet cells is regulated by Notch, Jak/STAT and Thyroid hormone signaling, and is accompanied by loss of MCC features, but not with increased apoptosis. **(A)** Schematic depiction of epidermal areas used for the analysis and quantification of MCCs in Fig. 3. Yellow boxes indicate areas used for MCC quantification in Fig. 3 A,B. Blue box indicates area used for MCC quantification in Fig. 3 C-F. Location of the dorsal lateral line is indicated in red. **(B)** Schematic summary of signaling events described in the context of mammalian airway MCC to Goblet cell trans-differentiation. **(C)** Schematic summary of signaling events that lead to MCC apoptosis and trans-differentiation described in this study. The targets of pharmacological intervention as well as the small molecules used in this study are depicted in red. Ruxo = Ruxolitinib. **(D,E)** De-acetylation of cilia, F-actin remodeling, loss of basal body polarity, and de-repression of proliferation in trans-differentiating MCCs. **(D)** Confocal micrographs of normal and trans-differentiating MCCs reveal disorganized basal bodies (Centrin4-GFP, green), cilia de-acetylation (Ac.-α-Tubulin, grey) and loss of basal body distal appendages (Cep164-mCherry) during MCC cilia retraction in the same specimen. Magnified areas are indicated by yellow boxes. **(E)** Quantification of MCC phenotypic differences between normal and trans-differentiating MCCs. N = number of MCCs. TD = trans-differentiating. χ^2 test, *** $P < 0.001$. Cf. Fig. 5 A,B. **(F)** Confocal micrographs of active Caspase 3 staining (magenta) in normal and trans-differentiating MCCs at stages 32-45 reveal lack of apoptosis marker in trans-differentiating MCCs. St. 32 N = 4; st. 41 N = 3; st. 45 N = 3 embryos.

Tasca et al. Fig. S6

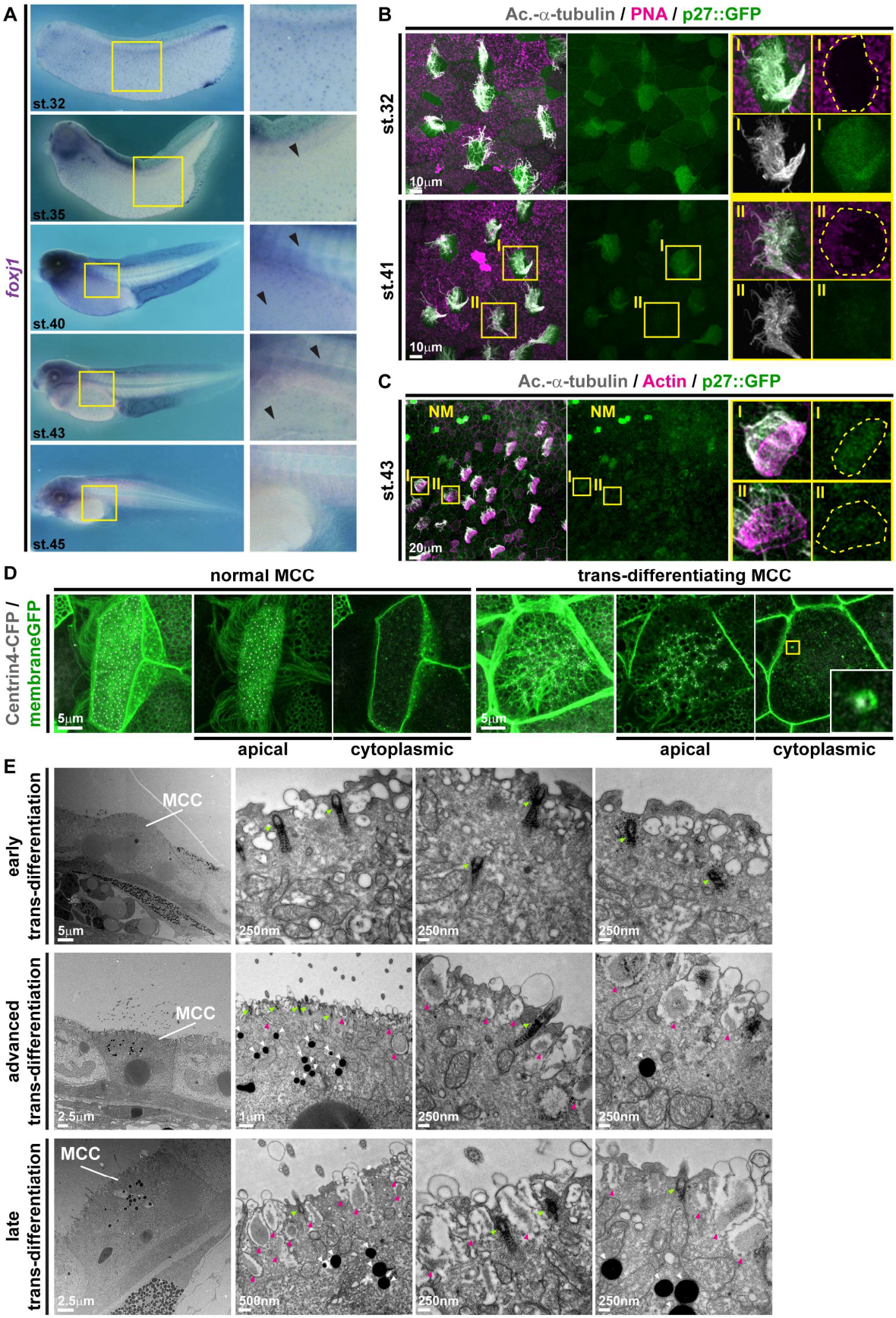

Supplemental Figure S6. (Related to Figure 5)

Loss of MCC-specific transcription and altered basal bodies in trans-differentiating MCCs. **(A)** *In situ* hybridization shows areas of progressive loss (black arrowheads) of *foxj1* (purple) expression in the epidermis of *Xenopus* tadpoles during stages (32 to 45) of MCC trans-differentiation. Yellow boxes indicate location of magnified images. St. 32 N = 14; st. 35 N = 12; st. 40 N = 10; st. 43 N = 4; st. 45 N = 8 embryos. **(B)** Confocal micrographs of transgenic p27::GFP (green) expression in normal and trans-differentiating MCCs at stages 32 and 41. MCCs (Ac.-α-Tubulin, grey), and mucus (PNA staining, magenta). Note the loss of GFP expression in MCCs with reduced cilia acetylation that start to express mucins as compared to normal MCCs within the same specimen. N = 3 embryos per stage. Magnified areas are indicated by yellow boxes. **(C)** Confocal micrograph of transgenic p27::GFP (green) expression in MCCs and Neuromasts (NM) at stage 43. MCCs (Ac.-α-Tubulin, grey), and F-actin (Actin, magenta). Note the loss of GFP expression in MCCs with reduced cilia acetylation and altered apical Actin as compared to less trans-differentiated MCC and Neuromast within the same specimen. N = 5 embryos. Magnified areas are indicated by yellow boxes. **(D)** Confocal micrographs of normal and trans-differentiating MCCs reveal cytoplasmic basal bodies (Centrin4-CFP, gray) co-localizing with membrane vesicles (membrane GFP, green) in late stage trans-differentiating MCC. Magnified area is indicated by yellow boxes. Note also the weakening of Centrin4-CFP signals per basal body in trans-differentiating MCC specimen. Normal MCCs, N = 7; trans-differentiating MCCs, N = 8; N = 3 embryos. **(E)** Transversal sections and transmission electron microscopy (TEM) of MCCs with different degrees of trans-differentiation (number of mucus granules; magenta arrowheads) show basal bodies (green arrowheads), including some localizing to the cytoplasm. Additionally, advanced and late trans-differentiating MCCs are enriched for lysosomes (white arrowheads). Multiple magnified images are shown, which are each derived from different section planes of the same MCC depicted in the left panel. N = 9 MCCs from 1 embryo.

Tasca et al. Fig. S7

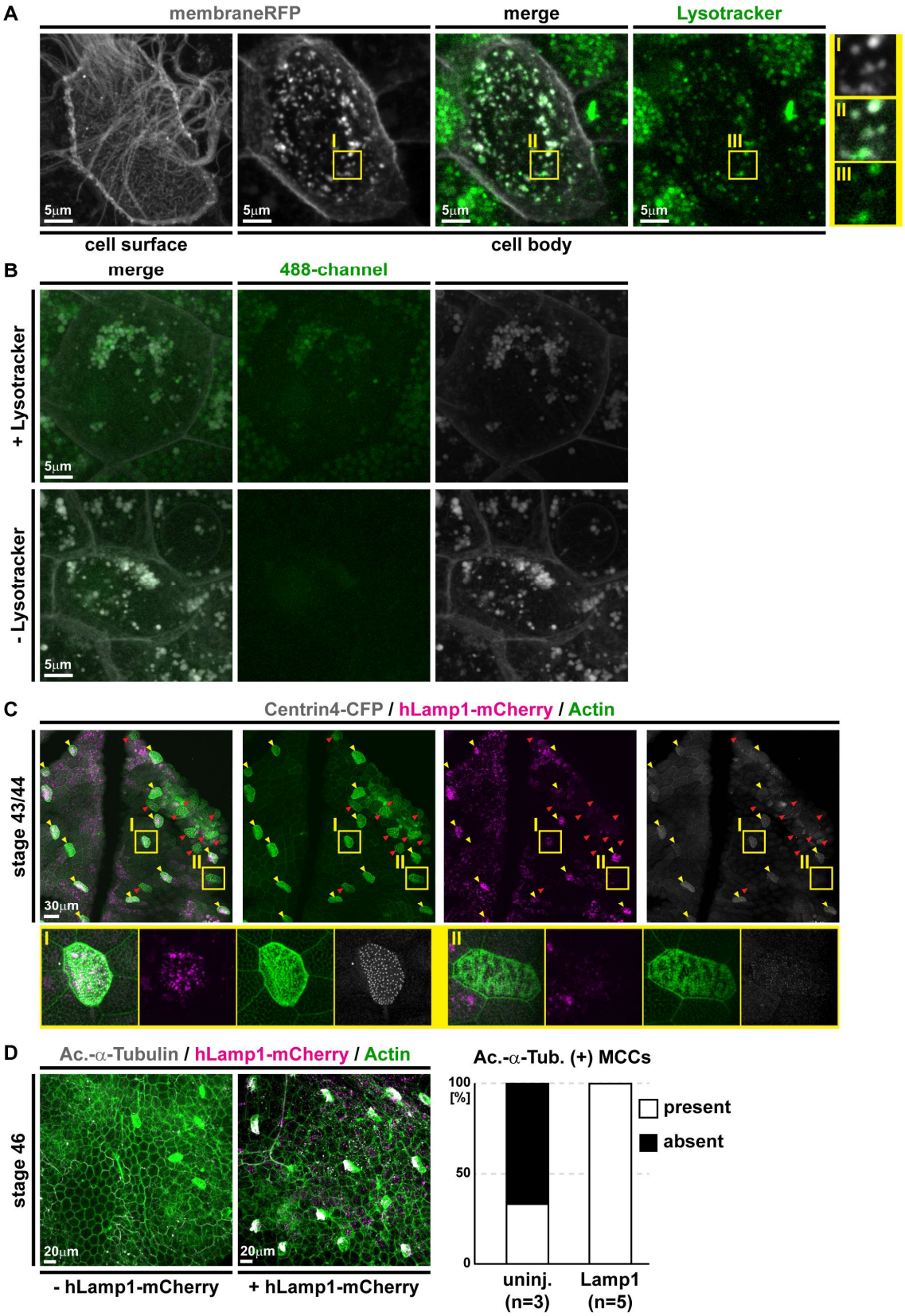

Supplemental Figure S7. (Related to Figure 5)

Tans-differentiating MCCs are enriched for lysosomes and Lamp1 overexpression interferes with trans-differentiation. **(A)** Confocal micrographs of trans-differentiating MCC reveal enrichment of cytoplasmic vesicles (mRFP, gray) that stain positive for Lysotracker (green). Magnified areas are indicated by yellow boxes. N = 33 MCCs / 11 embryos. **(B)** Comparison of 488-channel signals in Lysotracker treated (+Lysotracker) and non-treated (-Lysotracker) samples. Note also in A and B, that mucus granules in neighboring Goblet cells stain positive for Lysotracker, which is in line with mucus granule acidification required for Mucin packaging. **(C)** Confocal micrographs of normal and trans-differentiating MCCs within the same sample show enrichment of hLamp1-mCherry signals in targeted MCCs (yellow arrowheads) as compared to neighboring targeted Goblet cells. MCCs with hLamp1-mCherry overexpression do not show signs of trans-differentiation (yellow arrowheads) while trans-differentiation morphology is observed in non-targeted MCCs (red arrowheads). Sample was stained for Actin (F-actin, green). Magnified areas are indicated by yellow boxes. N = 48 MCCs / 4 embryos. Image was reconstructed from multiple individual micrographs. **(D)** Confocal micrographs of uninjected controls (-hLamp1-mCherry / uninj.) and hLamp1-mCherry injected (+ hLamp1-mCherry / Lamp1) specimens at st. 46. MCCs (Ac.-α-Tubulin, grey), hLamp1-mCherry (magenta), F-actin (Actin, green). hLamp1-mCherry injected tadpoles present ciliated MCCs, while uninjected controls are devoid of cilia. Uninjected N = 3 embryos / 2 Ac.- α-Tubulin (+) MCCs; hLamp1-mCherry injected N = 5 embryos / 61 Ac.- α-Tubulin (+) MCCs.